

V. READOUT

A. Relevance and Example

As discussed in section I, the quantum processor converts the initial state $|\psi(0)\rangle$ into a final state

$$|\psi_{fin}\rangle = c_0|0, 0, 0\dots 0\rangle + c_1|0, 0, 0\dots 1\rangle + c_2\dots$$

that contains the solution of the problem being investigated. The sum runs over all 2^N states, where N is the number of qubits.

According to this formal analysis, the result of the computation is contained in the 2^N coefficients c_i that determine the final state. However, the final result of any useful computation should have a numerical or Boolean logic value, such as *true* or *false* or 37. We therefore discuss here how to convert the final state of the computation (after the last unitary transformation) into the desired result.

Like the initialization process, the readout is a nonunitary operation that cannot be reversed: The wavefunction of the quantum register collapses during readout, becoming classical.

As an example readout process consider a function evaluation (such as in the Deutsch-Josza problem). Here the processing can be written as

$$|\psi_0\rangle = \sum_x |x, 0\rangle \Rightarrow |\psi_{fin}\rangle = \sum_x |x, f(x)\rangle,$$

where the superposition of all possible input states is transformed into a superposition of all possible input states and function values. As discussed in section IV, the goal of the DJ algorithm is to learn, with a single function call, whether a function is constant or balanced. Apparently the readout of the desired result from this superposition state is a nontrivial task.

Specializing to a single qubit, the algorithm starts with the superposition state of both input and output register

$$|\psi_0\rangle = |0\rangle|0\rangle - |1\rangle|0\rangle - |0\rangle|1\rangle + |1\rangle|1\rangle$$

After the function evaluation, this state is turned into

$$|\psi_1\rangle = |0\rangle|f(0)\rangle - |1\rangle|f(1)\rangle - |0\rangle|\bar{f}(0)\rangle + |1\rangle|\bar{f}(1)\rangle$$

if the two function values are the same, $f(0) = f(1)$, then

$$\begin{aligned} |\psi_{eq}\rangle &= |0\rangle|f(0)\rangle - |1\rangle|f(0)\rangle - |0\rangle|\bar{f}(0)\rangle + |1\rangle|\bar{f}(0)\rangle \\ &= (|0\rangle - |1\rangle)(|f(0)\rangle - |\bar{f}(0)\rangle), \end{aligned}$$

but if they are different, $f(0) \neq f(1) = \bar{f}(0)$,

$$\begin{aligned} |\psi_{ne}\rangle &= |0\rangle|f(0)\rangle - |1\rangle|\bar{f}(0)\rangle - |0\rangle|\bar{f}(0)\rangle + |1\rangle|f(0)\rangle \\ &= (|0\rangle + |1\rangle)(|f(0)\rangle - |\bar{f}(0)\rangle). \end{aligned}$$

In this trivial example, the type of measurement that must be performed is obvious: The input register is

in an eigenstate of σ_x . Its eigenvalue is +1 if the two possible function values are different (i.e. the function is balanced) or -1 if the two values are the same (i.e. the function is constant). Obviously the result can be determined from the single measurement of the variable I_x of qubit 1.

The example shows that (for a single qubit) a single measurement is sufficient to determine the result (constant or balanced). This power does not come for free: while one gains this ability, one loses the possibility to find out what these values are, i.e. whether the (constant) results are 0, 0 or 1, 1 or (for the case of a balanced function) $f(0) = 0$ and $f(1) = 1$ or $f(0) = 1$ and $f(1) = 0$.

The complete information that is contained in the final state are the 2^N coefficients c_i that define the superposition. Some sources claim that it is impossible to determine all these coefficients. This is not true, however, and we will give some examples for simple systems where this has been done. However, to determine all 2^N coefficients requires at least 2^N measurements, i.e. an effort that increases exponentially with the number of qubits. Obviously this is not possible without losing the advantage of quantum computers. Furthermore it can be difficult to make measurements that are state-selective, since such measurements must act on all N qubits simultaneously. Instead one usually is content with measurements on single qubits, which are often referred to as local measurements.

B. Quantum Mechanical Projection Postulate

The projection postulate is one of the fundamental assumptions on which quantum mechanics is based. It assumes that an ideal measurement brings a particle into the eigenstate ψ_i of the measurement operator A , where a_i is the corresponding eigenvalue, which we assume to be nondegenerate. We cannot predict in general which of the eigenstates will be realised, but the probability of the realisation of each state is

$$p_i = |\langle\psi_i|\psi_{fin}\rangle|^2$$

The observable that is used for this readout process must be adapted to the system used to implement the quantum computer as well as to the algorithm. A typical measurement would be the decision if qubit i is in state $|0\rangle$ or $|1\rangle$. The corresponding measurement operator may be written as S_z^i , i.e. as the z Pauli operator acting on qubit i , with (e.g.) the positive eigenvalue indicating that the qubit is in state $|0\rangle$ and the negative eigenvalue labeling state $|1\rangle$.

The usual treatment of measurement processes is due to von Neumann and is best pictured as a generalized Stern-Gerlach experiment: The measurement apparatus separates the particles according to their internal quantum states. In this picture it is obvious that the measurements are local, i.e. the results for the individual particles do not depend on the state of the other particles. Obviously the complete absence of interactions is not representative for a quantum computer.

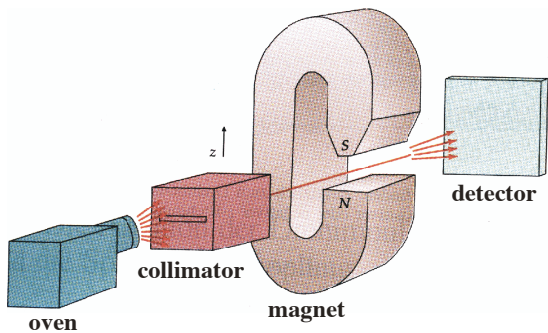


FIG. V.1: Stern-Gerlach experiment.

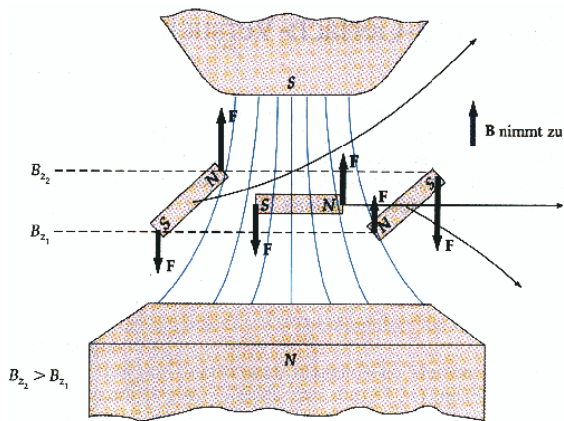


FIG. V.2: Pictorial representation of the coupling mechanism during the measurement process.

For this simple example, it is relatively straightforward to see how the inhomogeneous field separates the different particles according to their orientation: A particle whose north pole is closer to the south pole of the magnet has a lower energy than the particle with the opposite orientation - its potential energy is negative. It can further lower its energy by moving farther into the high field region and is therefore deflected upwards, while the oppositely oriented particle is deflected down. Transferred into the quantum mechanical context, particles will follow different trajectories depending on their spin state.

If we want to describe the result of a sequence of measurements, where different realizations of eigenstates may occur, it is more convenient to use a density operator description. Since the measurement projects the system into an eigenstate of the observable, the resulting density operator (which describes the ensemble of the measurement outcomes) is diagonal in the basis of these eigenstates. The measurement process corresponds to a nonunitary evolution

$$\rho \Rightarrow \sum_i A_i \rho A_i,$$

where the $A_i = |\psi_i\rangle\langle\psi_i|$ are the projection operators onto the eigenstates ψ_i of the observable A, i.e. op-

erators with a single 1 on the diagonal and zeroes everywhere else.

Apparently the measurement process simply eliminates all off-diagonal elements of the density operator in the basis of the observable (which is usually also an eigenbase of the Hamiltonian). This implies that the result of the measurement process will be a mixed state, unless the system was already in an eigenstate of A.

We will give some more details of the measurement process below; before that we put it in a historical and philosophical context.

C. The Copenhagen Interpretation

The conventional interpretation of this measurement process is due to Bohr and coworkers and known as the "Copenhagen Interpretation" of quantum mechanics. It can be summarised with a few fundamental assumptions (see Gif. V.3).

The Copenhagen Interpretation

- Quantum mechanics describes individual systems.
- Quantum mechanical probabilities are primry, i.e. they cannot be derived from a deterministic theory (like statistical mechanics)
- The world must be divided into two parts. The object under study must be described quantum mechanically, the remaining part, which includes the measurement apparatus, is classical. The cut between system and measurement apparatus can be made at an arbitrary position.
 - The observation process is irreversible.
- Complementary properties cannot be measured simultaneously.

Original Literature:

W. Heisenberg, 'Über den anschaulichen Inhalt der quantentheoretischen Kinematik und Mechanik', Z. Phys. **43**, 172-198 (1927).

N. Bohr, 'The quantum postulate and the recent development in atomic theory', Nature **121**, 580-590 (1928).

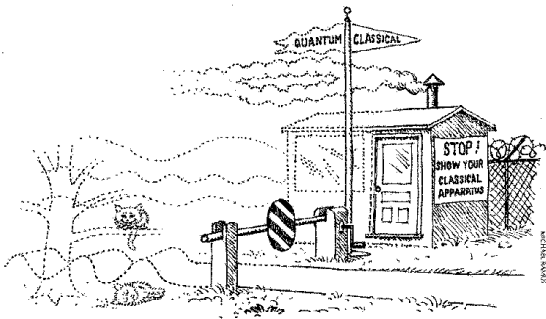
W. Heisenberg, 'Physik und Philosophie', Hirzel, Stuttgart (1958).

N. Bohr, Naturwissenschaftliche Rundschau **13**, 252-255 (1960).

FIG. V.3: Summary of the Copenhagen interpretation of the quantum mechanical measurement process.

The Copenhagen interpretation has the advantage that it is relatively simple and internally consistent. It cannot satisfy from an esthetic point of view, since it implies two different types of evolution: the "normal" unitary evolution of the Schrödinger equation and the nonunitary of the measurement process. In the strict sense, it implies that quantum mechanical systems cannot be attributed real properties; instead, it represents "only" a theory about the possible outcomes of measurements and their probabilities.

These deficiencies have prompted many researchers to look for better alternatives and / or to check some of the fundamental assumptions for their validity. A more detailed model that tries to integrate the measurement process with the unitary evolution under the



Aus W. Zurek, "Decoherence and the transition from quantum to classical," *Physics Today*, October 1991.

FIG. V.4: Separation of the world into a quantum mechanical / classical regions.

Schrödinger equation and avoids the splitting of the universe into a quantum mechanical and a classical part, is due to Johann von Neumann.

D. Von Neumann's Model

In his model, the system S is coupled to an apparatus A . For a simple 2-level system the basis states are ψ_a and ψ_b , the eigenstates of a system observable O_S . The measurement should determine if the system is in state ψ_a or ψ_b . To obtain a quantum mechanical description of the measurement process, we also describe the apparatus as a two-level system. The eigenstates are written as ξ_a and ξ_b and correspond to the apparatus indicating that the system is in state ψ_a and ψ_b , respectively. A corresponding observable acting on the apparatus can be written as O_A .

According to von Neumann, the measurement process involves coupling the system to the measurement apparatus through an interaction of the type

$$H_{int} = O_A B,$$

where O_A is the observable to be measured and B is a variable of the measurement apparatus. The system thus drives the motion of the measurement apparatus and in the idealized process, the eigenvalues of A can be read off a "pointer variable" of the measurement apparatus, which is treated classically. One usually assumes that the observable O_A that one tries to measure commutes with the Hamiltonian of the system. In the case of the Stern-Gerlach experiment, the observable O_A is the z -component of the spin operator S_z , and the pointer variable is the position z along the field direction.

Before the measurement process, the total (system and apparatus) can be described as a state without correlations between system and apparatus. The two parts can thus be described individually by the states $\psi = (c_a\psi_a + c_b\psi_b)$ (which is not known) and ξ and the combination by the product state

$$\psi \otimes \xi = (c_a\psi_a + c_b\psi_b) \otimes \xi$$

The interaction between system and apparatus must be such that it drives the evolution as

$$\psi_a \otimes \xi \rightarrow \psi_a \otimes \xi_a$$

and

$$\psi_b \otimes \xi \rightarrow \psi_b \otimes \xi_b$$

Since the evolution is linear, the superposition state evolves as

$$(c_a\psi_a + c_b\psi_b) \otimes \xi \rightarrow c_a\psi_a \otimes \xi_a + c_b\psi_b \otimes \xi_b.$$

Apparently the system is still in a superposition state, but it is now entangled between system and apparatus. Von Neumann's model does not generate a reduction of the wavepacket. This is a necessary consequence of the unitary evolution. The reduction only occurs if we assume in addition that the apparatus is a classical system, where a reduction **MUST** occur. A reduction of the wavefunction component for the apparatus into (e.g.) ξ_a then also causes a reduction of the system state into ψ_a .

While the wavefunction reduction is therefore not explained, it has been shifted farther away from the system. According to von Neumann's understanding, the final reduction occurs in the mind of the observer. While this is therefore not a full resolution of the measurement paradox, it improves the situation: Since the apparatus is very complex in terms of a quantum mechanical description, the collapse of its wavefunction is very fast. Furthermore, since it does not directly involve the system, some inconsistency is easier to accept. Nevertheless, one major issue remains unresolved in von Neumann's model (as well as in all others): We only obtain probabilities from the quantum mechanical description, i.e. we cannot predict the result of individual measurements.

An extension of the von Neumann measurement that is sometimes used in the context of quantum information processing and communication is the positive operator-valued measure (POVM), where the states that form the basis for the measurement are not orthogonal. The corresponding projection operators still must sum up to unity.

E. Entanglement

Entanglement (German: Verschränkung) is one of the characteristics of quantum mechanics that distinguishes it from classical physics. It describes the experimental fact that some properties of a quantum mechanical system cannot be described in terms of properties of independent, spatially separated subsystems, even if these subsystems do not interact.

While correlations between classical particles are well known, quantum correlations go beyond this. The best known type of correlations are those considered by Einstein Podolsky and Rosen in their famous paper [40] where they contended that quantum mechanics

was incomplete. It can be discussed classically: a particle that is at rest ($p = 0$) at position $x = 0$ decays into two equal particles. Conservation of momentum requires that these two particles move apart with opposite momentum ($p_1 = -p_2$), so that their position and momentum remain exactly anticorrelated for all times.

A better known variant of EPR correlations is due to Bohm and Aharonov [41] who proposed to use angular momentum components as noncommuting observables rather than momentum and position. In their example, two photons (e.g.) are created in a singlet state and move apart. If any spin component is measured on the two particles, the results will always be anticorrelated.

While this type of correlations exist in classical systems also (we have no problems understanding the example given), there are quantum correlations that have no classical analog. In the system defined by Aharonov and Bohm, one has to measure spin components on both particles with analysers that are not in the same orientation to find these correlations.

A prescription for a measurement of quantum correlations that has no classical analog was given by John Bell [42, 43]. For this purpose, one has to make three or more measurements at different angles between zero and ninety degrees. For such an arrangement, he could prove an inequality that must be satisfied for all classical systems, but which is violated by quantum mechanics.

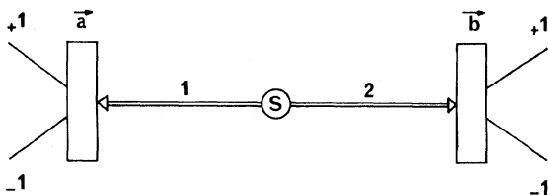


FIG. V.5: Correlation experiment for the derivation of Bell's inequality.

Rather than discuss the original Bell inequality, we briefly mention the version that was introduced by Clauser, Horne, Shimony and Holt [44]. The consider (see figure) two photons that are generated in a singlet state. They pass individually through polarising beam splitters, whose orientation can be set individually, and the outputs are defined as having eigenvalues ± 1 .

The measurement results are described by the joint probabilities $P_{++}(\vec{a}, \vec{b})$, where \vec{a} and \vec{b} denote the orientation of the two analysers and P_{++} the frequency of measuring $+$ for both particles. Similarly one defines $P_{+-}(\vec{a}, \vec{b})$, $P_{-+}(\vec{a}, \vec{b})$, and $P_{--}(\vec{a}, \vec{b})$.

The correlation of the two measurements is then defined as

$$E(\vec{a}, \vec{b}) =$$

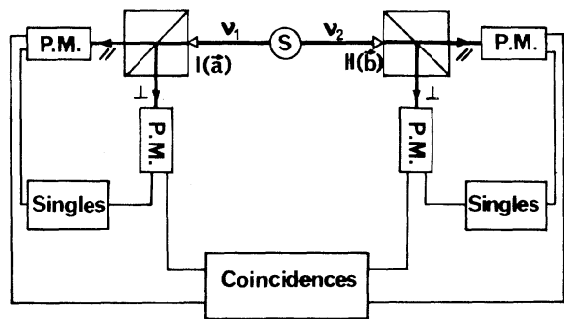


FIG. V.6: Measurement of correlation coefficients.

$$P_{++}(\vec{a}, \vec{b}), +P_{--}(\vec{a}, \vec{b}) - P_{+-}(\vec{a}, \vec{b}) - P_{-+}(\vec{a}, \vec{b}),$$

i.e. as the difference between equal and opposite results.

Choosing two different orientations \vec{a} and \vec{a}' for particle 1 and \vec{b} and \vec{b}' for particle 1, Bell defined the function

$$S = E(\vec{a}, \vec{b}) - E(\vec{a}, \vec{b}') + E(\vec{a}', \vec{b}) + E(\vec{a}', \vec{b}')$$

Using classical probability theory, Bell could show that for classical particles, the function S must satisfy the inequality

$$-2 \leq S \leq 2,$$

independent of the orientation of the analysers.

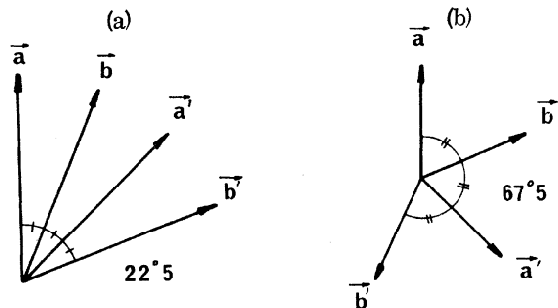


FIG. V.7: Choice of orientations that maximize the violation of Bell's inequality.

Quantum mechanics (and experiment) violate this inequality, however: for the specific choice

$$\alpha = 0^\circ, \alpha' = 45^\circ, \beta = 22.5^\circ, \beta' = 67.5^\circ,$$

one obtains

$$S = -2\sqrt{2} < -2,$$

in contradiction to Bell's inequalities.

The prediction was verified experimentally by a number of groups, most notably by Alain Aspect [45], who used photon pairs that were created in a singlet state by an atomic cascade.

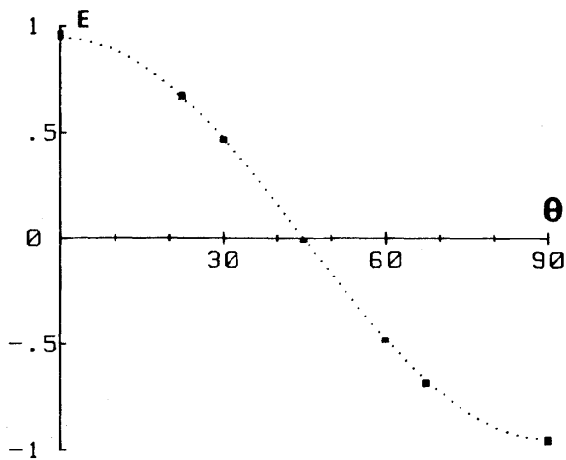


FIG. V.8: Quantum mechanical prediction (curve) and experimental result (dots) for correlation coefficient.

The entanglement of different qubits can make it difficult to extract the information. Consider, e.g., a maximally entangled state like

$$|\psi\rangle = \frac{1}{\sqrt{2}}(|00\rangle + |11\rangle).$$

Any measurement on a single qubit on this state will give completely random results, i.e. no information. The entanglement therefore hides the information for local measurements.

F. Measurement Strategies

Most quantum algorithms require a readout of the state of each qubit independent of all other qubits. This readout should provide a reliable information of the final state. As discussed above, this will not allow a complete determination of the state. Consider, r.g., the two states

$$|\psi_1\rangle = \frac{1}{\sqrt{2}}(|00\rangle + |11\rangle).$$

and

$$|\psi_2\rangle = \frac{1}{2}(|00\rangle + |01\rangle + |10\rangle + |11\rangle).$$

They will in 50% of all cases yield $|0\rangle$ and in the other 50% one if the qubits are measured independently. Obviously the two cases can be distinguished by taking correlations into account: In the first case, measurements on the individual spins always yield the same result; in the second case, they are completely uncorrelated.

Experimental readout schemes can never be 100% efficient, since photons may be lost, detectors have noise or dark counts. One therefore should be able to repeat the measurement to increase the probability for correct results. The main difficulty for this is that every

measurement changes the state of the system: as discussed above, after the measurement the system is no longer in the state that resulted from the computation, but in a mixed state. It is therefore not immediately obvious that a second measurement yields the same result.

Several strategies are possible to circumvent this problem: one can try to use a QND (=quantum nondemolition measurement). Such a measurement arranges for the unavoidable influence that the measurement must have on the qubit to be such that it does not affect later measurements of the same variable. Not all variables can be measured this way, but in most cases it should be possible to arrange the system in such a way that QND measurements can be used at least in principle.

Another possibility is to read out not the qubit itself, but a copy of it. If the measurement is not successful, or to check the validity of the measurement result, one can then make an additional copy and read that out. Such a procedure could be repeated many times to achieve very reliable readout even with very unreliable single measurements.

The critical part here is the copy operation, which must be reliable. As we have stressed before, it is not possible to clone a quantum mechanical state, i.e. to make a perfect copy. However, copying just the information of a quantum mechanical state that is relevant for the readout of a specific variable is perfectly possible (in principle!) and can be repeated arbitrarily often. As an example, the operation

$$CNOT|x, 0\rangle = |x, x\rangle \quad \text{for } x = 0, 1$$

copies the first bit into the second, which must be initialized to zero.

If the qubit $|q\rangle$ is in a superposition state

$$|q\rangle = a|0\rangle + b|1\rangle = \begin{pmatrix} a \\ b \end{pmatrix},$$

it is coupled to a measurement qubit $|m\rangle = |0\rangle$ to the product state

$$|q\rangle|m\rangle = (a|0\rangle + b|1\rangle)|0\rangle = \begin{pmatrix} a \\ 0 \\ b \\ 0 \end{pmatrix},$$

and the CNOT operation turns it into

$$CNOT \begin{pmatrix} a \\ 0 \\ b \\ 0 \end{pmatrix} = \begin{pmatrix} a \\ 0 \\ 0 \\ b \end{pmatrix} = (a|0\rangle|0\rangle + b|1\rangle|1\rangle).$$

A measurement can now be performed either on the qubit $|q\rangle$ itself or on the measurement qubit $|m\rangle$. If the measurement yields a result (i.e. finds that the measurement qubit is in state $|0\rangle$ or $|1\rangle$), it collapses the wavefunction of both qubits simultaneously. If it does not provide a result, one has the option of

discarding the qubit. This corresponds to eliminating its degrees of freedom and leaves the qubit in the state

$$|q\rangle = a'|0\rangle + b'|1\rangle = \begin{pmatrix} a' \\ b' \end{pmatrix},$$

which is almost equal to the original state. The difference between the coefficients $a' = ae^{i\phi_a}$ and $b' = be^{i\phi_b}$ of this final state and the coefficients before the copy operation is that the readout of the measurement qubit $|m\rangle$ changes the phase of the coefficients a and b by arbitrary values. It does not, however, change the absolute values $|a'|^2 = |a|^2$ and $|b'|^2 = |b|^2$ and therefore the probabilities for later measurement attempts.

G. Ion Traps

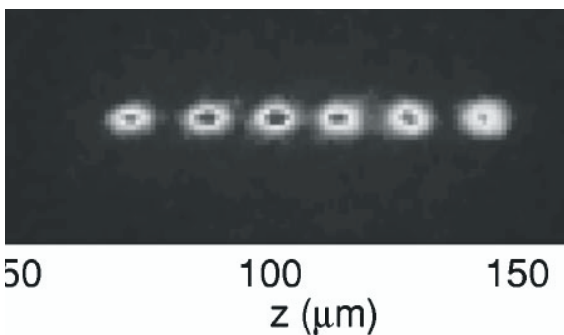


FIG. V.9: Ions in a linear trap.

Atomic ions permit a relatively straightforward readout provided the qubit has been properly identified. As the figure shows, the ions are (relatively) easily distinguished. Identification of the qubits is by their position in the trap. Compared to the picture, an actual readout has to make the fluorescence state-selective: one wants, e.g., to see only those ions that are in the $|0\rangle$ state.

Since the lifetime of the states that are used for storing the quantum information must be large, they do not emit radiation spontaneously. However, an excellent possibility is to excite the atom from the state that is to be measured to an electronically excited state from where it can emit a photon, which can be detected as a signature of the atom having been in the corresponding ground state.

Since the detection efficiency for a single photon is relatively low, it is unlikely that a single photon absorption leads to a detection. It is therefore necessary to repeatedly scatter photons from the atom. Since the procedure must also be selective, the procedure requires that the atom always returns into the original state; the individual measurement can then be considered a QND process, since it does not affect the relevant observable, i.e. the population of the atomic state, although it completely randomises its phase.

The figure shows a typical atomic level scheme for an alkali atom or earth alkali ion, containing a large number of allowed transitions. A transition that assures

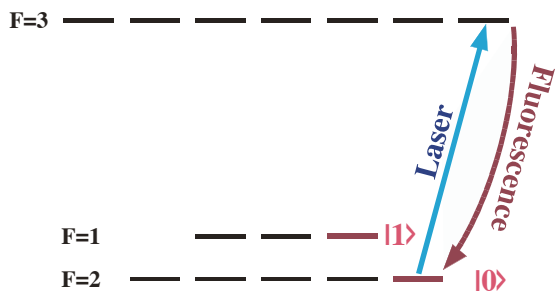


FIG. V.10: Example of a cycling transition for the measurement of state $|0\rangle$.

that the atom returns to the initial state after absorption of a photon and is therefore suited for a QND measurement is known as a cycling transition: the ion is cycled repeatedly through the same pair of levels, each time scattering a photon from the laser beam. In the example shown in the figure, such a transition can be realized for the $|0\rangle = |F = 2, m_F = 2\rangle$ state by irradiating it with circularly polarized light: the atom can only absorb light from the circularly polarised laser beam by going to the excited $|F = 3, m_F = 3\rangle$ state. Similarly, the excited state can only decay to state $|0\rangle$, since all other transitions are forbidden by angular momentum conservation. If the number of such cycles is high enough, the state of the atom can be detected with high probability.

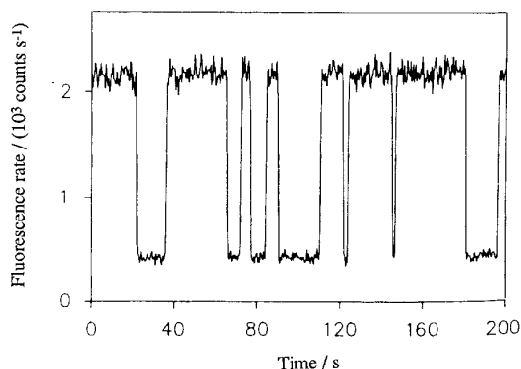


FIG. V.11: Quantum jumps indicate changes of the internal quantum state of the ion.

The detection scheme sketched here only provides a measure of the atom being in state $|0\rangle$; a similar measurement of state $|1\rangle$ is not possible for the level scheme shown in the figure. The complementary measurement of the atom being in state $|1\rangle$ can be achieved in different ways. The first possibility is to take the absence of a result for the state $|0\rangle$ measurement as a measurement of the atom being in state $|1\rangle$. This is possible since the system (under ideal conditions) *must* be either in state $|0\rangle$ or state $|1\rangle$. A second possibility is to perform first the measurement of state $|0\rangle$ and then apply a logical NOT operation and a second measurement of state $|0\rangle$. Since the NOT oper-

ation interchanges the two states, a subsequent measurement of the state $|0\rangle$ is logically equivalent to a measurement of state $|1\rangle$ before the NOT operation.

H. The Quantum Zeno Effect

Zeno of Elea (ca. 490 - 430 b.C., southern Italy) was a student of Parmenides. He stated a number of paradoxes to defend the teachings of Parmenides, in particular the statement that motion is impossible and more than one thing cannot exist. One well known paradox is that of the race between Achilles and the tortoise. Achilles (the fastest man in antiquity) is ten times as fast as the tortoise. Nevertheless he cannot overtake her if she gets a head start of (e.g.) 10 m: Achilles first must cover these 10 m. During this time, the tortoise moves 1 m and is therefore still ahead. While he covers this meter, the tortoise moves another 0.1 m and so on, always staying ahead.

Another motion paradox "proves" that a body cannot move from A to B: for this, it would first have to move to the middle of the distance. For this it first would have to move to the middle of the first half etc.

While these paradoxes are easily resolved, similar situations exist in quantum mechanics that are real. They have been discussed under the heading "quantum Zeno effect", although they cannot really be considered paradoxes.

We consider the evolution of a state that is initially (at $t=0$) prepared into the state $|\psi_i\rangle$, which is an eigenstate of operator A with eigenvalue a_i . The state evolves under the influence of a Hamiltonian H , which does not commute with A . A possible example would be that the Hamiltonian is $\propto I_z$ and the observable is I_x . A measurement with A of the system after some time τ will then in general yield a result that is different from a_i .

For the spin system, we can consider a spin in the $m_x = +1/2$ eigenstate of I_x evolving in a magnetic field $B_0||z$. The probability that a subsequent measurement at time t also finds the eigenvalue $+1/2$ is then

$$p_+ = \frac{1}{2}(1 + \cos(\omega_L t)),$$

while the probability to obtain the opposite result is

$$p_- = \frac{1}{2}(1 - \cos(\omega_L t)).$$

If such a measurement is performed, the projection postulate states that after the measurement the system is in an eigenstate of A . If the measurement yielded the result $+1/2$, the system is again in the same initial state, and the evolution starts out again with the same time dependence. The important point is that the first derivative of the time dependence,

$$\frac{d}{dt}p_+|_{t=0} = 0$$

vanishes after the projection: the system therefore does not change during short times. If the measurement is repeated on a time scale that is fast compared

to the Larmor precession, the actual evolution can therefore be described as a quasi-linear process, with the time scale determined by the product of Larmor frequency and measurement interval.

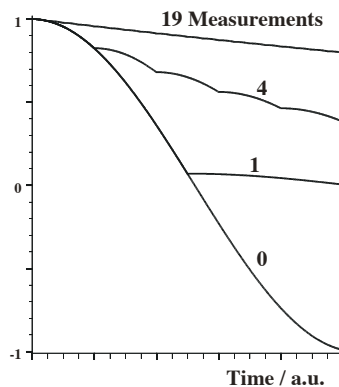


FIG. V.12: Quantum Zeno effect: the decay of a state becomes slower with the number of readouts.

As the measurement interval decreases, the evolution of the system becomes quasi-linear. If a series of measurements is repeated with a separation (in time) of τ , the probability that n measurements in sequence will always find the system in state $m_x = +1/2$ becomes

$$p_+ = \frac{1}{2}(1 + \cos(\omega_L \tau))^n.$$

For short measurement intervals, $\omega_L \tau \ll 1$ this can be expanded as

$$p_+ \approx \left(1 - \frac{\omega_L^2 \tau^2}{4}\right)^n.$$

Using the expansion

$$(1 - \epsilon)^n \simeq e^{-n\epsilon}$$

the time evolution can be written as

$$p_+(n\tau) = p_+(t) = e^{-\frac{\omega_L^2 \tau}{4} t}.$$

The evolution is not only slower, it is also damped: The system no longer shows precession, but moves exponentially towards thermal equilibrium.

These general quantum mechanical predictions can be verified experimentally e.g. for trapped ions [46]. Here, the state of the ion was measured by fluorescence: the laser for the excitation of the fluorescence was switched on for the n measurements and the fluorescence was measured. With increasing number of such measurements, a drastic decrease of the transition probability was found.

Clearly the slow-down of transition rates by measurement cannot be universal. As an example consider an atom that is initially in the excited state. A possible measurement for the excited state population probability is a fluorescence measurement: as long as we do not observe a fluorescence photon from this atom, we know it is still in the excited state. If we only "look"

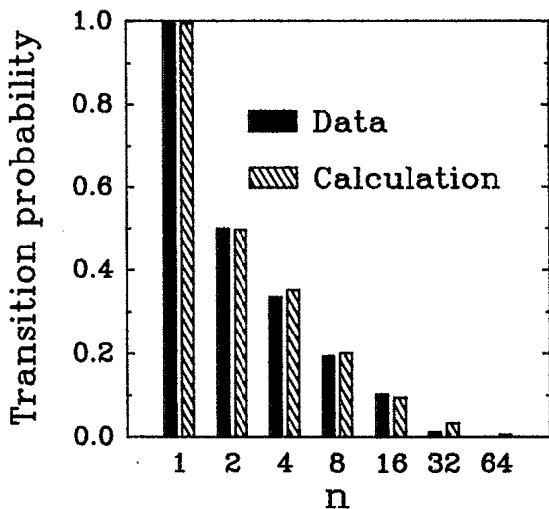


FIG. V.13: Quantum Zeno effect: slowing of transitions for trapped ions.

at the atom often enough, it is therefore impossible for the atom to decay. Similar arguments are used to explain why the decay of the proton has not yet been observed.

The main reason for this paradox is that the concept of a quantum mechanical measurement is not established with sufficient precision. A projection, i.e. a reduction of the wavepacket, does not always occur in "standard" QM measurements. If the interaction is weak (such as "looking" for a fluorescence photon), the reduction does not occur. One important point that must be considered is that an projective measurement can only occur during a finite time interval, which is longer the weaker the coupling to the apparatus is. The projection postulate is well suited to the Stern-Gerlach type experiment, but completely unsuitable for experiments like NMR.

I. NMR

Detection of precessing Magnetization by Faraday Effect

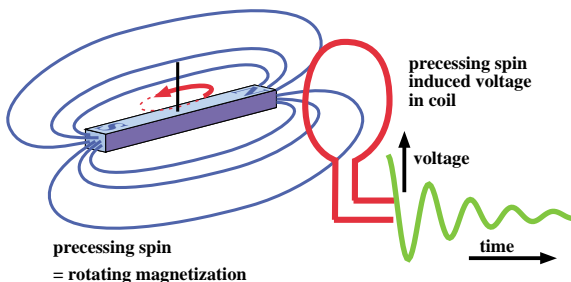


FIG. V.14: Experimental detection of transverse magnetization in NMR.

Detection in magnetic resonance is best described in a classical picture: the transverse components of the

spin generate a macroscopic magnetisation that precesses around the static magnetic field. The magnetic flux through a coil oriented perpendicular to the field changes therefore sinusoidally. According to Faraday's law, such a temporal variation in the magnetic flux induces a voltage in the coil, which is recorded as the signal.

Obviously such a detection scheme is not compatible with the usual description of a quantum mechanical measurement, which involves the collapse of a wavefunction. Instead, one observes the system continuously, without significantly affecting its behavior. This difference is closely related to the fact that the system is an ensemble, rather than the usually assumed single particle system. In addition, the observed quantity is not the population of some state, i.e. $\langle \psi_k | \psi_k \rangle$, but rather the evolution of a coherence, i.e. $|\psi_j \rangle \langle \psi_k|$.

There are cases in quantum computation, where the readout process hinges on the collapse of a wavefunction. For those cases, which include Shor's algorithm, the algorithm must be modified when it is applied to an NMR system. The non-existence of a collapse is handled by appending an additional step, which is polynomial in the number of bits and allows one to obtain the result from ensemble measurements.

When a quantum algorithm requires the measurement of populations, it can be trivially modified to allow implementation on an NMR quantum computer: It is straightforward to convert populations into coherences that are directly proportional to the populations and are directly observable.

Before we discuss these possibilities, we first check which quantities are directly observable. The state

$$\frac{1}{\sqrt{2}}(|0\rangle + |1\rangle) \otimes |0\rangle$$

contains observable coherence (i.e. transverse magnetization), but not the state $|0\rangle$ or the state $|1\rangle$. While the instantaneous observable is $\sum_i I_x^i$ or $\sum_i S_y^i$, we need to take into account that a NMR measurement is not instantaneous; rather, one measures an FID signal over a total time of about a second. During this period, the Zeeman part of the Hamiltonian turns I_x and I_y into each other:

$$H_z : I_x \rightarrow I_y \rightarrow -I_x \rightarrow -I_y \rightarrow I_x.$$

Similarly, the coupling Hamiltonian causes evolutions of the type

$$H_{IS} : I_x \rightarrow I_x(t) = e^{-i\phi I_z S_z} I_x e^{i\phi I_z S_z} = I_x \cos\phi + I_y S_z \sin\phi$$

The resonance lines observed in an NMR spectrum correspond to measures of the coherence in the allowed transition, which are determined by the conditions that

$$\Delta m_i = \pm 1, \Delta m_j = 0, i \neq j$$

one spin changes its magnetic quantum number, all other spins remain. If other components of the density operator are to be measured, this is possible by converting them into observable magnetization.

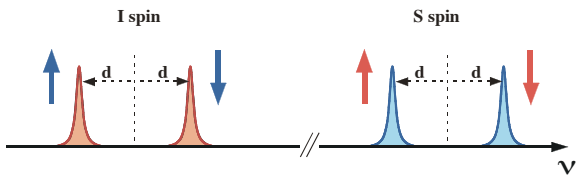


FIG. V.15: Spectrum for two weakly coupled spins.

J. Measurements on Multi-Spin Systems

In a coupled spin system, as is used in NMR quantum computing, one observes in general 2^N resonance lines, which all contain information about the quantum mechanical state.

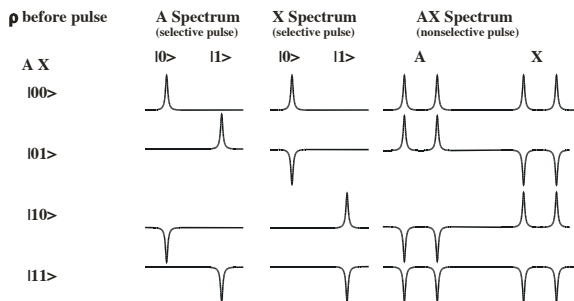


FIG. V.16: Signals in NMR readout for different spin states.

As an example of the NMR readout, we consider the AX system.

In a weakly coupled two-spin system, every transition can be labeled with its spin and the state of the other spin. The figure shows how the logical states of the qubits can be turned into observable magnetization by radio frequency pulses. The combination of the initial state and the type of radio frequency pulses determines the pattern of amplitudes in the observed spectrum. A selective pulse is a pulse that affects only one spin, while the other spins remain unaffected. RF pulses are always selective between different types of nuclei, but they can be made selective or nonselective for nuclei of one species in different chemical environments.

A selective $e^{-i\pi/2A_x}$ or $e^{-i\pi/2A_y}$ rf pulse turns the state $|00\rangle$ into observable coherence

$$\frac{1}{\sqrt{2}}(|0\rangle + |1\rangle)|0\rangle$$

of the A spin. Similarly a $e^{-i\pi/2X_x}$ or $e^{-i\pi/2X_y}$ rf pulse turns it into observable coherence

$$\frac{1}{\sqrt{2}}|0\rangle(|0\rangle + |1\rangle)$$

of the X spin. If the initial state is $|10\rangle$, the same signals are observed on the A spin, but with opposite phase. On the X spin, this initial state generates a

positive signal, but in the opposite transition. Similar observations are possible for the $|01\rangle$ and $|11\rangle$ states.

In NMR one often prefers to write the passive spin not in terms of occupied states, but as spin operators S_x , S_y , or S_z as basis operators for the expansion of the density operator. The coherence of a single transition can then be written as

$$\rho_{12} + \rho_{21} = (1 + I_z) \otimes S_x.$$

Similarly the other S-spin transition corresponds to coherence

$$\rho_{34} + \rho_{43} = (1 - I_z) \otimes S_x.$$

The sum of the two transitions is therefore

$$\rho_{12} + \rho_{21} + \rho_{34} + \rho_{43} = 1 \otimes S_x.$$

Similarly we can take the difference, which corresponds to one of the two lines in emission:

$$\rho_{12} + \rho_{21} - \rho_{34} - \rho_{43} = I_z \otimes S_x,$$

which is the quantity that results from the coupled evolution.

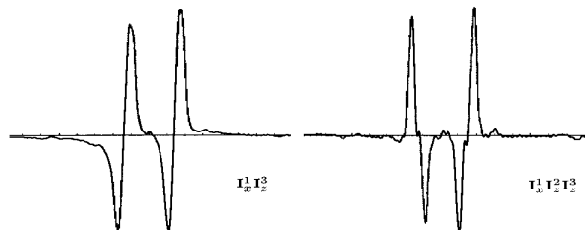


FIG. V.17: Examples of observed spectra for specific density operator components.

Some examples of the observed signals are summarized in the figure. Obviously the system used here is not ideally suited for quantum computing: the resonance lines are not fully resolved, indicating that decoherence is active before a computation can be finished. This scheme can easily be extended to more spins.

K. Quantum State Tomography

The single FID and associated spectra apparently provide 2^N numbers as a result, equal to the number of coefficients in an N spin system. The density operator of the system contains additional information (e.g. about the effect of decoherence, which can be measured by an extension of this scheme. This procedure is called "quantum state tomography", in reference to X-ray tomography, where a sequence of two-dimensional pictures is taken to reconstruct the 3D body being imaged.

The coherences that are directly observable with this scheme are single quantum coherences with $\Delta m =$

± 1 . Higher order ($\Delta m > 1$) and zero quantum coherences ($\Delta m = 0$) do not generate an observable signal. To make them observable, one can use radio frequency pulses to transfer them into other elements of the density operator.

A systematic approach to measuring the full density operator is described by Chuang et al. [47, 48]: The simplest quantum state tomography procedure on a two spin system involves nine runs, in which each nucleus is either (i) left undisturbed, (ii) rotated with a $(\frac{\pi}{2})_x$ pulse or (iii) rotated with a $(\frac{\pi}{2})_y$ pulse. As one measures four resonance lines after each readout sequence, one obtains a total of 36 amplitudes, which suffice to determine the 16 density operator elements.

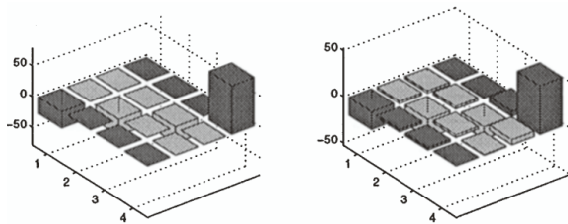


FIG. V.18: Theoretical and experimental density operator components during Grover experiment.

The figure shows a comparison between the experimental and theoretical density operator elements during a Grover search experiment [47]. Clearly the highest population is found for the $|11\rangle$ state.

L. Single spin readout

Single spin readout is not possible in liquid state NMR, but has been achieved in solids [49, 50].

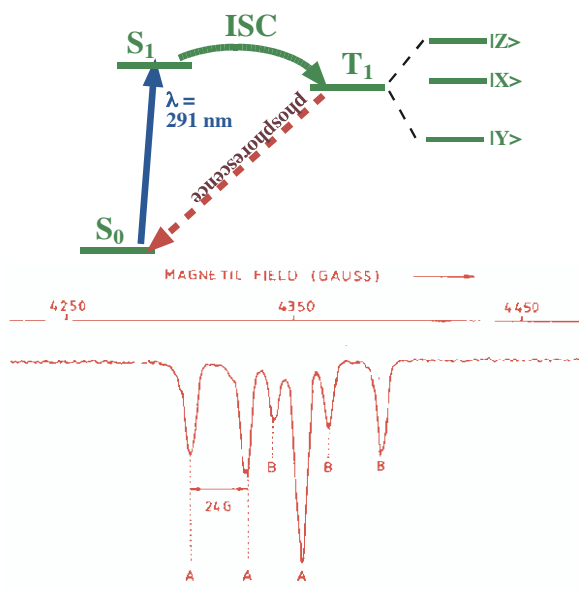


FIG. V.19: Schematics of optically detected magnetic resonance.

A much larger number of examples for single spin detection has been published for electron spin resonance (EPR) [49, 50, 51, 52, 53, 54]. These experiments typically use fluorescence detection, in close analogy to the state-selective detection experiments of trapped ions. A laser drives a transition from the singlet ground state to an optically excited triplet state. Intersystem crossing transfers some of the population into the long-lived triplet state. The fluorescence yield depends on the spin state of intermediate triplet states; if states with long lifetimes become populated, the fluorescence yield drops; it can be re-established by irradiating the spins with a suitable radio-frequency / microwave source. When the frequency matched a transition between the triplet states, the system can undergo a transition from the long-lived triplet state to another state with a shorter lifetime and fall back into the ground state from there. In the example spectrum, the microwave frequency was kept constant while the magnetic field was scanned to bring different transitions into resonance with the microwave frequency.

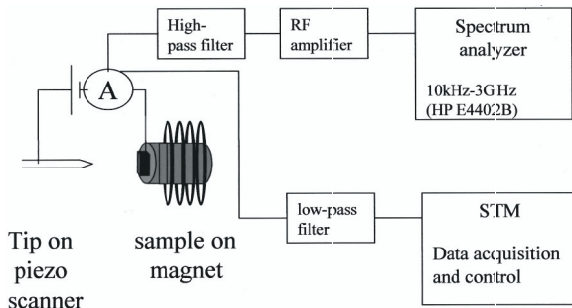


FIG. V.20: Schematics of setup for STM-detected EPR.

Another experimental approach to single spin detection uses an scanning tunneling microscope (STM) [55, 56]. While the details of the experiment must be considered unknown, it appears that the tunneling current contains an oscillating component at the Larmor frequency if the tip is placed over a paramagnetic molecule. The oscillating signal component is separated from the dc component and fed into a microwave spectrum analyzer.

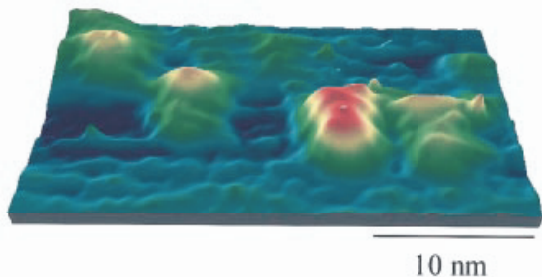


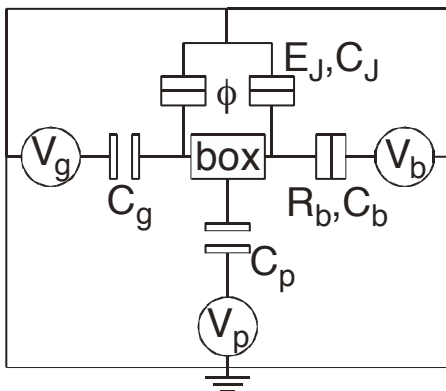
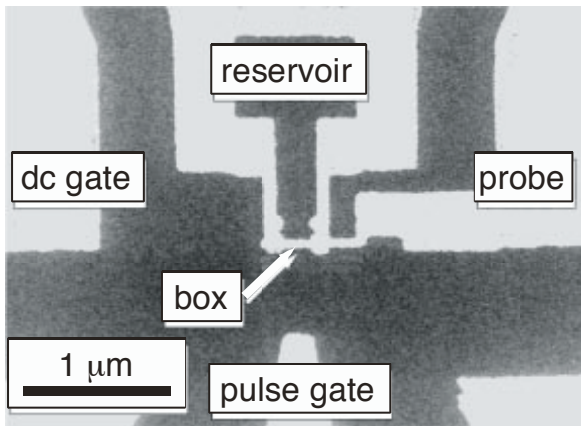
FIG. V.21: Spatial distribution of STM-EPR signal on Si surface. The red areas correspond to adsorbed molecules.

By setting the detection frequency to the EPR fre-

quency, it is possible to map the spin density on the surface. In this example [56], an organic radical BDPA was deposited on a graphite surface. The images show individual BDPA molecules.

Both techniques - optical and STM-EPR allow the detection of individual electronic spins. While this is not a readout of the spin state, it can be used as such if the spin being detected is not the qubit to be read out, but coupled to the computational qubit: the coupling shifts the EPR frequency, allowing one to detect the spin state of the computational qubit through the EPR frequency of the readout qubit.

M. Superconducting qubits



 : tunnel junction
 : capacitor

FIG. V.22: Superconducting qubit.

Superconducting qubits typically contain dots or rings isolated by Josephson junctions [57]. The two logical states are distinguished either by a charge or by an additional flux quantum. In this example, the qubit is defined by the two lowest energy states of the "box". They differ by a Cooper pair, i.e. by a charge $2e$. The relative energy can be tuned by the gate electrode. The tunnel process through the Josephson junction to the reservoir corresponds to a coupling between the two pure charge states. If the gate is adjusted to

match the energies of the pure charge states, the tunneling creates a coherent exchange between them. A coherent superposition of the two states can be created by initialization of the system into the ground state and then suddenly pulsing the pulse gate to equalize the energy of the two states. Leaving them in the degenerate states for a quarter of the tunneling cycle time creates an equal superposition of the two states. Readout can be performed for the charge-type quantum dots by an SET, which is very sensitive to small changes in the electric field or by a SQUID, which detects small changes in magnetic flux. In the system of Nakamura et al., the probe electrode was used for readout. It is coupled to the box by a tunnel junction, which provides an escape route for excess electrons in the box: if an excess Cooper pair is in the box, a tunnel current is registered through the probe gate. This electrode is also used to initialize the system into the ground state. Since the coupling is an efficient source of decoherence for the system, it will have to be switched off for an actual quantum information processing device.

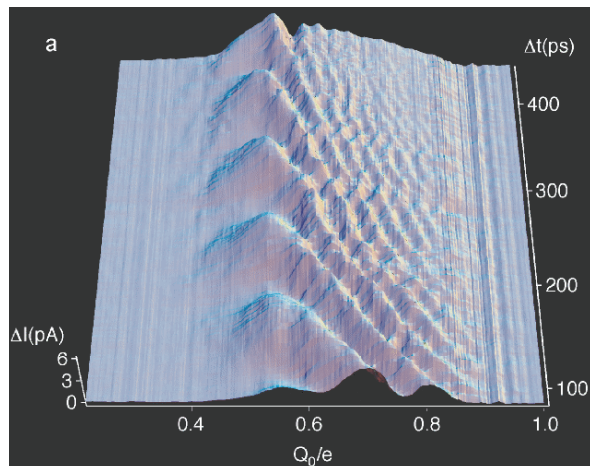


FIG. V.23: Signal from superconducting qubit undergoing Rabi oscillations as a function of control charge.

In the system displayed in the figure, Rabi oscillations have been initiated with an intense electrical field pulse. Variants of superconducting qubits have also been implemented that are intermediate between the charge and flux qubit. While the readout is done on a single system, it represents an average over a large number of pulse cycles. The measured quantity was therefore the probe current, not the number of electrons. It is proportional to the probability of finding the qubit in the upper state. The oscillation period is given by the tunnel splitting, which can be tuned with the flux ϕ through the loop that includes the two tunnel junctions between the reservoir and the box. It agrees with the splitting that was measured by microwave spectroscopy. At larger offsets, the cycle Rabi frequency increases, but the oscillation amplitude decreases. To reduce noise, the experiment was performed at a temperature of 30 mK in a dilution refrigerator.

N. Semiconductor qubits

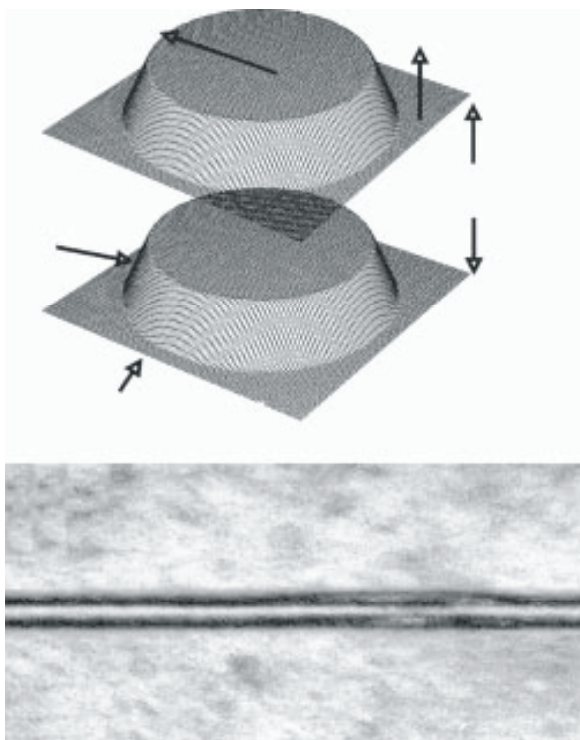


FIG. V.24: Two coupled quantum dots as qubits; top: schematic representation; bottom: transmission electron micrograph; height of dots is 1-2 nm, dot separation 4 nm, dot radius 8-12 nm.

Semiconductor qubits are still at a very early stage [58, 59], since no reports of coherent control have been published yet. Most suggestions on the use of semiconductors start with quantum dots, i.e. semiconductor structures whose dimensions are of the order of 5-50 nm in all three dimensions.

One way of building such structures is by depositing a semiconductor material on a substrate with a different lattice constant. The usual example is the growth of InAs on a substrate of GaAs. The difference in lattice constant implies that the material grown on top is significantly strained. The elastic energy associated with this strain can be minimized if the layer grows not as a film, but assembles into islands; this process is called Stranski-Krastanow growth.

Stopping the growth process at the right moment leaves an assembly of mesa-like structures behind, whose dimensions can be adjusted to match the range where quantum confinement effects are significant. If additional layers of GaAs and InAs are grown over the quantum dots, the dots in the second layer tend to align with the existing dots. One has therefore a good chance to obtain coupled dots, as in the example shown in the figure.

In this example, two qubits are encoded by correlated electron-hole states in two qubits that are separated by 4-8 nm. The two qubits are represented by an electron and a hole. They can be located in either of

the two quantum dots. The tunnel effect couples these two localized states into symmetric and antisymmetric linear combinations, which may be used as the logical states of the qubits.

Measurements on single quantum systems are rather straightforward, since the photoemission by quantum dots is rather high. However, the readout must be state-selective, and readout of the result depends therefore on the implementation chosen.

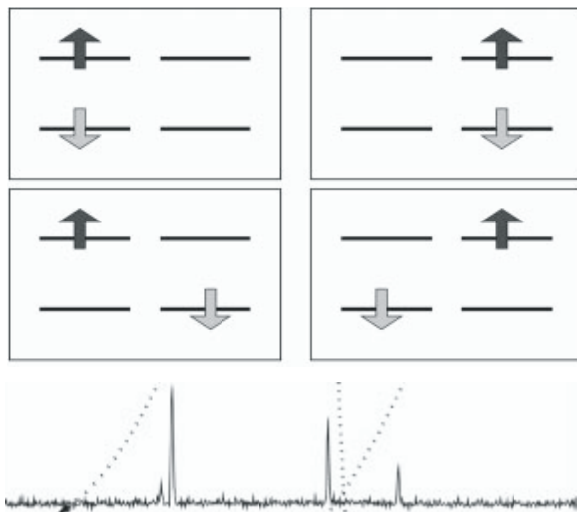


FIG. V.25: The logical state of two qubits is encoded in the photoemission wavelength. In this example, only three of the four states are visible.

Since the different states have different energies, they can be distinguished by the photoemission wavelength. Only three of the four states are visible in this example.

While this scheme provides a relatively easy and reliable readout, it is clearly not a scalable readout scheme, since the number of resonance lines increases exponentially with the number of qubits. Furthermore, the readout is achieved for single dots, but it is not a single-instance readout: only a small number of the electron-hole pairs recombine such that photons are created and picked up by the detection system. Overall a large number of absorption-emission events must occur until a significant signal is detected.

Separation between different quantum dots must be of the order of the optical wavelength to allow one to distinguish between different qubits by far field optics. A larger number of qubits, which corresponds to a sizeable quantum register would therefore have inter-qubit separations that are too large for significant couplings.

VI. QUANTUM GAMES (BY KAVITA DORAI)

Quantum version of the prisoner's dilemma. Idea by Eisert et al., PRL **83**,3077(1999), experimental implementation using NMR with two protons in cytosine by Du et al., PRL **88**,137902(2002).

-
- [1] Michael Brooks. *Quantum Computing and Communications*. Springer, New York, 1999. 152 pp. IA
- [2] Jozef Gruska. *Quantum computing*. McGraw-Hill, London, 2000. 439 pp. IA
- [3] Michael A. Nielsen and Isaac L. Chuang. *Quantum computation and quantum information*. Cambridge Univ. Press, Cambridge, 2001. 676 pp. IA, IA, IIB, IIC, IVC 1, IVC 1, IVE 1, IVE 1, IVE 2, IVE 3, IVE 3
- [4] Colin P. Williams and Scott H. Clearwater. *Explorations in quantum computing*. Springer, New York, 1998. 307 pp, CD-ROM, DM 98.00. IA
- [5] A. Steane. Quantum computing. *Rep. Prog. Phys.*, 61:117–173, 1998. IA
- [6] Dorit Aharonov. Quantum computation. In Dietrich Stauffer, editor, *Annual Reviews of Computational Physics VI*, pages 259–346. World Scientific, 1999. Preprint quant-ph/9812037. IA
- [7] A. Galindo and M. A. Martin-Delgado. Information and computation: Classical and quantum aspects, 2002. *Rev. Mod. Phys.*, to appear. Preprint quant-ph/0112105. IA, IV A, IVC 2, IVE 3
- [8] John Preskill. Quantum computation. <http://theory.caltech.edu/preskill/ph229/>, 1997. 413 pp. IA
- [9] Paul Benioff. Quantum mechanical Hamiltonian models of Turing machines. *J. Stat. Phys.*, 29:515, 1982. ID
- [10] Richard P. Feynman. Simulating physics with computers. *Int. J. Theor. Phys.*, 21:467–488, 1982. ID
- [11] Peter Shor. Polynomial-time algorithms for prime factorization and discrete logarithms on a quantum computer. In *Proceedings, 35th Annual Symposium on Foundations of Computer Science*, Piscataway, NJ, 1994. IEEE Press. IE, IV A
- [12] W.K. Wootters and W.H. Zurek. A single quantum cannot be cloned. *Nature*, 299:802–803, 1982. IG
- [13] D. Dieks. Communication by EPR devices. *Phys. Lett. A*, 92:271–271, 1982. IG
- [14] D.P. DiVincenzo. The physical implementation of quantum computation. *Fortschr. Phys.*, 48:771–783, 2000. Preprint quant-ph/0002077. IL
- [15] A. Einstein. Zur Quanten-Theorie der Strahlung. *Phys. Zeitschrift*, 18:121–128, 1917. IIID
- [16] R. Frisch. Experimenteller Nachweis des Einsteinschen Strahlungsrückstosses. *Z. Physik*, 86:42–48, 1933. IIID
- [17] F. Mintert and C. Wunderlich. (title). *Phys. Rev. Lett.*, 87:257904, 2001. IIIG, IIIL
- [18] Th. Sauter, R. Blatt, W. Neuhauser, and P.E. Toschek. Quantum jumps observed in the fluorescence of a single ion. *Optics Commun.*, 60:287–292, 1986. IIHH
- [19] T.W. Hänsch and A.L. Schawlow. Cooling of gases by laser radiation. *Optics Commun.*, 13:68–69, 1975. IIH
- [20] D. Wineland and H. Dehmelt. Proposed 10-14 laser fluorescence spectroscopy on tl^+ mono-ion oscillator iii. *Bull. Am. Phys. Soc.*, 20:637, 1975. IIH
- [21] W. Neuhauser, M. Hohenstatt, P. Toschek, and H. Dehmelt. Optical-sideband cooling of visible atom cloud confined in parabolic well. *Phys. Rev. Lett.*, 41:233–236, 1978. IIH
- [22] D.J. Wineland, R.E. Drullinger, and F.L. Walls. Radiation-pressure cooling of bound resonant absorbers. *Phys. Rev. Lett.*, 40:1639–1642, 1978. IIH
- [23] S. Chu, L. Hollberg, J.E. Bjorkholm, A. Cable, and A. Ashkin. Three-dimensional viscous confinement and cooling of atoms by resonance radiation pressure. *Phys. Rev. Lett.*, 55:48–51, 1985. IIH
- [24] C. Monroe, D. M. Meekhof, B. E. King, W. M. Itano, and D. J. Wineland. (title). *Phys. Rev. Lett.*, 75:4714, 1995. IIK
- [25] B.E. King, C.S. Wood, C.J. Myatt, Q.A. Turchette, D. Leibfried, W.M. Itano, C. Monroe, and D.J. Wineland. (title). *Phys. Rev. Lett.*, 81:1525, 1998. IIK, IIIL
- [26] C. A. Sackett, D. Kielpinski, B. E. King, C. Langer, V. Meyer, C. J. Myatt, M. Rowe, Q. A. Turchette, W.M. Itano, D. J. Wineland, and C. Monroe. (title). *Nature*, 404:256, 2000. IIK
- [27] H. C. Nägerl, D. Leibfried, H. Rohde, G. Thalhammer, J. Eschner, F. Schmidt-Kaler, and R. Blatt. (title). *Phys. Rev. A*, 60:145, 1999. IIK
- [28] Ch. Roos, Th. Zeiger, H. Rohde, H. C. Nägerl, J. Eschner, D. Leibfried, F. Schmidt-Kaler, and R. Blatt. (title). *Phys. Rev. Lett.*, 83:4713, 1999. IIK
- [29] J. I. Cirac, P. Zoller, H. J. Kimble, and H. Mabuchi. (title). *Phys. Rev. Lett.*, 78:3221, 1997. IIIL
- [30] L. Grover. (title). In *Proc. 28th Annual ACM Symposium on the Theory of Computation*, pages 212–219, New York, 1996. ACM Press. IV A, IVE
- [31] L.K. Grover. Quantum mechanics helps in searching for a needle in a haystack. *Phys. Rev. Lett.*, 79:325–328, 1997. Preprint quant-ph/9706033. IV A, IVE
- [32] D. Deutsch. Quantum theory, the Church-Turing principle and the universal quantum computer. *Proc. Roy. Soc. London A*, 400:97, 1985. IV B
- [33] D. Deutsch and R. Jozsa. Rapid solution of problems by quantum computation. *Proc. Roy. Soc. London A*, 439:553, 1992. IV B
- [34] R. Cleve, A. Ekert, C. Macchiavello, and M. Mosca. Quantum algorithms revisited. *Proc. Roy. Soc. London A*, 453:339–354, 1998. IV B
- [35] J.M. Myers, A.F. Fahmy, S.J. Glaser, and R. Marx. Rapid solution of problems by nuclear-magnetic-resonance quantum computation. *Phys. Rev. A*, 63:032302, 2001. IV B
- [36] A. Ekert and R. Jozsa. Quantum computation and Shor’s factoring algorithm. *Rev. Mod. Phys.*, 68:733–753, 1996. IVC 1, IVC 1
- [37] L. Vandersypen, M. Steffen, G. Breyta, C.S. Yannoni, M.H. Sherwood, and I.L. Chuang. Experimental realization of Shor’s quantum factoring algorithm using nuclear magnetic resonance. *Nature*, 414:883–887, 2001. IVD, IVD 2, IVD 3
- [38] Lov K. Grover. Quantum computing. *The Sciences*, July/August:24–30, 1999. IVE 1
- [39] N. Bhattacharya, H. B. van Linden van den Heuvell, and R. J. C. Spreeuw. Implementation of quantum search algorithm using classical Fourier optics. *Phys. Rev. Lett.*, 88:137901, 2002. IVE 3
- [40] A. Einstein, B. Podolsky, and N. Rosen. Can quantum mechanical description of physical reality be considered complete? *Phys. Rev.*, 47:777, 1935. VE
- [41] D. Bohm and Y. Aharonov. Discussion of experimental proof for the paradox of einstein, rosen, and podolsky. *Phys. Rev.*, 108:1070–1076, 1957. VE

- [42] J.S. Bell. On the einstein podolsky rosen paradox. *Physics*, 1:195–200, 1964. VE
- [43] N.D. Mermin. Hidden variables and the two theorems of john bell. *Rev. Mod. Phys.*, 65:803, 1993. VE
- [44] J.F. Clauser, M.A. Horne, A. Shimony, and R.A. Holt. Proposed experiment to test local hidden-variable theories. *PRL*, 23:880–884, 1969. VE
- [45] Alain Aspect, Philippe Grangier, and Grard Roger. Experimental tests of realistic local theories via bell's theorem. *Phys. Rev. Lett.*, 47:460–463, 1981. VE
- [46] W.M. Itano, D.J. Heinzen, J.J. Bollinger, and D.J. Wineland. Quantum zeno effect. *Phys. Rev. A*, 41:46:2295, 1990. VH
- [47] Isaac L. Chuang, Neil Gershenfeld, and Mark Kubinec. Experimental implementation of fast quantum searching. *prl*, 80:3408–3411, 1998. VK, VK
- [48] I.L. Chuang, N. Gershenfeld, M.G. Kubinec, and D.W. Leung. Bulk quantum computation with nuclear magnetic resonance: theory and experiment. *Proc. Roy. Soc. Lond. A*, 454:447–467, 1998. VK
- [49] J. Wrachtrup, A. Gruber, L. Fleury, and C. von Borczyskowski. Magnetic resonance on single nuclei. *cpl*, 267:179–185, 1997. VL, VL
- [50] D. Gammon, Al. L. Efros, T. A. Kennedy, M. Rosen, D. S. Katzer, D. Park, S. W. Brown, V. L. Korenev, and I. A. Merkulov. Electron and nuclear spin interactions in the optical spectra of single gaas quantum dots. *prl*, 86:5176–5179, 2001. VL, VL
- [51] J. Köhler, J.A.J.M. Disselhorst, M.C.J.M. Donckers, E.J.J. Groenen, J. Schmidt, and W.E. Moerner. Magnetic resonance detection of a single molecular spin. *Nature*, 363:242–243, 1993. VL
- [52] J. Wrachtrup, C. von Borczyskowski, J. Bernard, M. Orrit, and R. Brown. Optical detection of magnetic resonance in a single molecule. *Nature*, 363:244–245, 1993. VL
- [53] J. Köhler. Magnetische resonanz an einzelnen molekülen. *Phys. Bl.*, 52:699–702, 1996. VL
- [54] Jürgen Köhler. Magnetic resonance of a single molecular spin. *Physics Reports*, 310:261–339, 1999. VL
- [55] Y. Manassen, I. Mukhopadhyay, and N. Ramesh Rao. Electron-spin-resonance stm on iron atoms in silicon. *prb*, 61:16223–16228, 2000. VL
- [56] C. Durkan and M. E. Welland. Electronic spin detection in molecules using scanning-tunnelingmicroscopy- assisted electron-spin resonance. *Appl. Phys. Lett.*, 80:458–460, 2002. VL, VL
- [57] Y. Nakamura, Yu. A. Pashkin, and J. S. Tsai. Coherent control of macroscopic quantum states in a single-cooper-pair box. *Nature*, 398:786–788, 1999. VM
- [58] Gang Chen, N. H. Bonadeo, D. G. Steel, D. Gammon, D. S. Katzer, D. Park, and L. J. Sham. Optically induced entanglement of excitons in a single quantum dot. *Science*, 289:1906–1909, 2000. VN
- [59] M. Bayer, P. Hawrylak, K. Hinzer, S. Fafard, M. Korukusinski, Z. R. Wasilewski, O. Stern, and A. Forchel. Coupling and entangling of quantum states in quantum dot molecules. *Science*, 291:451–453, 2001. VN